ISSN No: 2348-4845
International Journal & Magazine of Engineering, Technology, Management and Research
A Peer Reviewed Open Access International Journal

Aircraft Gas Turbine Blade Response Analysis for High Cycle Fatigue

Jino K John
Department of Mechanical Engineering
Malla Reddy College of Engineering and Technology, Maisammaguda, Dhulapally Post, Secunderabad-500100, India.

Mr. D. Mangeelal
Department of Mechanical Engineering
Malla Reddy College of Engineering and Technology, Maisammaguda, Dhulapally Post, Secunderabad-500100, India.

ABSTRACT

High cycle fatigue has been a serious engineering problem in many industries since 1800's. The fracture on a turbine blade of a turbojet has been investigated to see the crack initiation. The turbine blade had initially cracked by a fatigue mechanism over a period of time and then fractured by the overload at the last moment. The fracture on turbine blade is located at top fir tree root and the fracture surface exhibits two characteristic zones, the first zone shows slow and stable crack growth with crystallographic faceted cracking and striation formation, and the second shows interdendritic fracture typical of final stage failure.In this paper the simulation of the turbine blade behavior is carried out using finite element software ANSYS for simulating the blade in fatigue analysis. Since the turbine blade is fixed to the rotor, the nodes at the lower end of the blade are constrained in all DOF and subjected to high frequency vibratory loading. With these boundary and load condition the number of cycle to failure is determined.

Keywords: ***Turbine blade failure, High cycle fatigue,thermal fatigue, FEM***

INTRODUCTION

Fatigue has not always been a technical subject or consideration in the disciplines of solid mechanics or strength of materials. Fatigue is not a technical subject that has been around hundreds of years. In fact, it came into being in the 1800s because of numerous accidents associated with railroad axles and railroad bridges, both of which were subjected to repeated loading. Although the terminology "high cycle fatigue" (HCF) was not used in connection with these accidents and the subsequent investigations, the high cycle counts associated with some of these incidents put them in the high cycle category. Most of the early papers on fatigue dealt with tests to failure and an attempt to establish an endurance limit, a term now associated with HCF.

On a conventional stress-life curve, commonly called a S–N curve or a Wöhler diagram, HCF occurs at the right end of the curve where the number of cycles is usually too large to be able to obtain sufficient statistically significant data to be able to characterize the material behavior with a very high degree of confidence.

The diagram used most commonly in low cycle fatigue(LCF) is generally referred to as an S–N curve which is a plot of maximum stress (S) as a function of number of cycles to failure (N) as depicted in Figure 1.1(a). This diagram is also referred to as a stress-life curve or a Wöhler diagram, after the famous scientist August Wöhler who conducted the first extensive series of fatigue tests and is often referred to as the father of fatigue. The diagram is drawn for test data obtained at a constant value of stress ratio, R. For each value of R, a different curve is drawn. Many attempts have been made and models developed to consolidate data at different values of R with a single parameter based on combinations of stress amplitude and maximum stress or other functions of stress.

Cite this article as: Jino K John & Mr. D. Mangeelal, "Aircraft Gas Turbine Blade Response Analysis for High Cycle Fatigue", International Journal & Magazine of Engineering, Technology, Management and Research, Volume 5 Issue 1, 2018, Page 57-62.

ISSN No: 2348-4845
International Journal & Magazine of Engineering, Technology, Management and Research
A Peer Reviewed Open Access International Journal

For HCF, the emphasis is on the value of stress at the fatigue limit and the data are represented on a Goodman diagram which is a plot of alternating stress against mean stress as shown in Figure 1.1(b). Each value of R is represented as a straight line drawn radially outward from the origin and the plot is the locus of points having a constant life in the HCF such as 10^7 cycles.

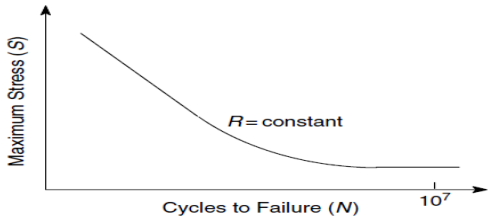

Fig 1.1 (a) S–N curve for LCF Fig 1.1

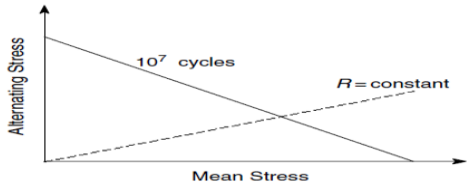

Fig 1.1 (b) Goodman diagram for HCF

Critical components, for which safe operating lives aredefined, include the major rotating parts, the turbo machinerydisks and shafts, and structural casingssubjected to high loads. In addition to the majorcomponents, other components in the rotating assemblies,such as spacers, cover-plates and seals, may also bedesignated as critical. To avoid unacceptable risk ofcatastrophic failure it is necessary to monitor the life usageof critical components and retire them from service beforetheir allocated life has been exceeded.

LITERATURE SURVEY

Numerical stress and crack initiation analysis of the compressor bladesafter foreign object damage subjected to high-cycle fatigue, LucjanWitek, 2011.[1]

Inference:

The shoot peening introduces the compressive (residual)stress into the surface layer of the material. Superposition of the actual (tensioned) stress with the residual (compressed)stress causes that the fatigue life of the shoot peened components is larger.

Keynote:

A non-linear finite element method was utilized to determine the stress state of the blade during the first mode of transverse vibration.

Failure analysis of a gas turbine compressor, G.H. Farrahi, M. Tirehdast, E. Masoumi Khalil Abad,S. Parsa , M. Motakefpoor, 2010.[2]

Inference:

- Analysis showed that multiple cracks had been initiated in the interfaceof the disks and shaft by the fretting fatigue mechanism and had been propagated by fatiguemechanism.
- Fatigue cracks were initiated at the interface of the shaft and the disks by fretting fatigue mechanism and propagate the fatigue mechanism.

Keynote:

Increasing of the vibration amplitude of the rotor near the second natural frequency of the rotor were the probable sources of the applied unusual loading condition on the compressor rotary components.

Failure analysis of Ti6Al4V gas turbine compressor blades, A. Kermanpur, H. Sepehri Amin , S. Ziaei-Rad, N.Nourbakhshnia, M.Mosaddeghfarc, 2007.[3]

Inference:

- SEM fractographyshowed different aspects of fretting fatigue including multiple crack initiation sites, fatigue beach marks, debrisparticles, and a high surface roughness in the edge of contact (EOC).
- Failure has occurred due to the tight contactbetween the blade root and the disk in the dovetail region as well as low wear resistance of the blade root.

Keynote:

The high level of stress at the contact surface can be due to the insufficient clearance between the blade root and the disk in the dovetail region. This lead to the complete failure of the blade.

ISSN No: 2348-4845
International Journal & Magazine of Engineering, Technology, Management and Research
A Peer Reviewed Open Access International Journal

Failure due to structural degradation in turbine blades, N. Ejaz, A. Tauqir , 2005.[4]

Inference:

- When the cracks approached critical lengths, the tipswere fractured leaving transgranular islands on the fracture surface.
- Failure sensitive cracks are present in other regions of the airfoil.Microstructural degradation has taken place in both the blades.

Keynote:

The cause of failure is found to be intergranular cracks, which started during exposure to high temperature. [5]

MATHEMATICAL ANALYSIS OF TURBINE BLADE

VELOCITY TRIANGLE:

From the velocity triangles, applying the principle of angular momentum of the rotor, the stage work output per unit mass flow is given by

$$W_s = U(C_{w2} + C_{w3}) = UC_a(\tan\alpha_2 + \tan\alpha_3) \quad (5.1)$$

From the steady flow energy equation we have

$$W_s = c_p \Delta T_{0s}, \quad (5.2)$$

Where ΔT_{0s} is the stagnation temperature drop in the stage, and hence

From the equation (5.1) & (5.2)

$$c_p \Delta T_{0s} = UC_a(\tan\alpha_2 + \tan\alpha_3) \quad (5.3)$$

Temperature equivalent of inlet & outlet velocity is given by

$$T_{0s} - T_s = \frac{{C_s}^2}{2C_p} \quad (5.4)$$

Considering the temperature in axial direction is constant, ($T_{01} = T_{02} = 1500$ K).

From the above equations, the temperature at the inlet & outlet of the blade 1430.12 K & 1356.07 K is determined.

TURBINE BLADE SKETCH:

In general gas turbine engines contains series of High Pressure Blade and Low Pressure Blade. In turbine compounding have an increasing order from high pressure, intermediate pressure & low pressure.

Figure 4.1 shows commonly used fir tree root fixing which permits replacement of blades. The fir trees are made easy fit in the trim, being prevented from axial momentum only (e.g. by a lug on one side and peening on the other).when the turbine is in running, the blade are held firmly in separation by centripetal force, but the slight freedom to move can provide a useful source of damping for unwanted vibration.

From blade design data, the diameter of the turbine blade section,

D_{tip} = 0.6972 m

D_{root} = 0.5334 m

1	Inlet absolute angle (α_2)	63.5^0
2	Inlet relative angle (β_2)	43.3^0
3	Outlet absolute angle (α_3)	18.4^0
4	Outlet relative angle (β_3)	50.51^0

Table 4.1 Blade inlet & outlet air angles.

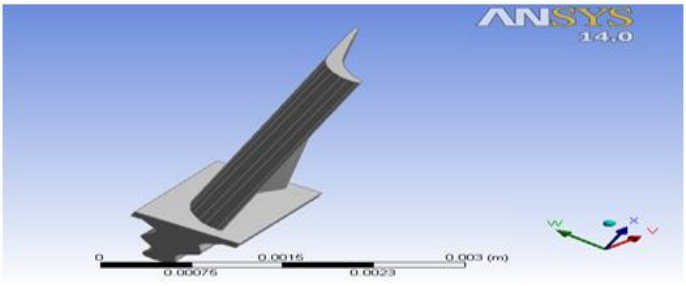

Figure 4.1 High Pressure Turbine blade sketch

MESHED MODEL:

Mesh generation is one of the most critical aspects of engineering simulation. Too many cells may result in long solver runs, and too few may lead to inaccurate results. ANSYS Meshing technology provides a means to balance these requirements and obtain the right mesh for each simulation in the most automated way possible. ANSYS Meshing technology has been built on the

ISSN No: 2348-4845
International Journal & Magazine of Engineering, Technology, Management and Research
A Peer Reviewed Open Access International Journal

strengths of stand-alone, class-leading meshing tools. The strongest aspects of these separate tools have been brought together in a single environment to produce some of the most powerful meshing available.

The highly automated meshing environment makes it simple to generate the following mesh types:

- Tetrahedral
- Hexahedral
- Prismatic inflation layer
- Hexahedral inflation layer
- Hexahedral core
- Body fitted Cartesian
- Cut cell Cartesian

Consistent user controls make switching methods very straight forward and multiple methods can be used within the same model. Mesh connectivity is maintained automatically.

Different physics requires different meshing approaches. Fluid dynamics simulations require very high-quality meshes in both element shape and smoothness of sizes changes. Structural mechanics simulations need to use the mesh efficiently as run times can be impaired with high element counts. ANSYS Meshing has a physics preference setting ensuring the right mesh for each simulation.

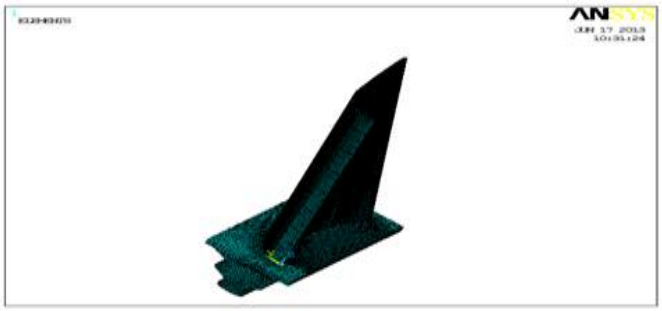

Figure 7.6 Meshed model

Hexahedral elements (bricks) can be used to mesh regularly shaped rectangular type volumes, while tetrahedral elements (tets) can be used to mesh any volume.Parametric geometry finite model of the turbine blade is shown above, which consists of 70725 nodes and 101871 SOLID 45 elements.

RESULTS AND DISCUSSION

In this analysis, the load is applied as a repeated cyclic loading of various time intervals into two events at two types of different repetitions of varying temperature.

SL.NO	POSITION	NODE	NODE LOCATION			TEMP (K)
			X	Y	Z	
1	ROOT-LE1	2653	0.05	0.002	0	1412
2	ROOT-LE2	4504	0.05	0.002	0.1	1412
3	ROOT-LE3	4503	0.05	0.002	0.2	1412
4	ROOT-LE4	4502	0.05	0.002	0.3	1411
5	ROOT-TE1	2683	1.39	0.019	0	1398
6	ROOT-TE2	3050	1.39	0.189	0.1	1398
7	ROOT-TE3	3049	1.39	0.189	0.2	1397
8	ROOT-TE4	3048	1.39	0.189	0.3	1397
9	ROOT-MDL1	2655	0.8	0.22	0	1406
10	ROOT-MDL2	4323	0.8	0.218	0.1	1406
11	ROOT-MDL3	4322	0.8	0.218	0.2	1406
12	ROOT-MDL4	4321	0.8	0.218	0.3	1405
13	MIDDLE	4080	0	0.346	6.279	1423
14	TIP-LE	4063	0	0.336	9.0	1430
15	TIP-TE	3051	1.34	0.168	9.0	1356

Table 8.1 Temperature distribution at various nodes

Due to the convection and conduction, the temperature varies from the LE to TE and from root to tip of the turbine blade. The temperature distribution along the various nodes is shown in the table 8.1. The result shows the temperature is maximum near the LE and minimum near the LE.

Number of cycles used

Cumulative fatigue usage (CFU) = $n_1/N_1 + n_2/N_2$

Event 1, n = 10^6cycles and Event 2, n = 10^4 cycles:

SL.NO	NODE	ALTERNATIVE STRESS (MPa)		CYCLES USED/ALLOWED		CFU
		EVENT 1	EVENT 2	n_1/N_1	n_2/N_2	
1	2653	2.5192	3.1491	0.4721	0.0351	0.5072
2	4504	4.6123	5.7650	0.17505	0.03943	0.21448
3	4503	3.1617	3.9521	0.001	0.0002	0.0012
4	4502	3.7396	4.6746	0.00927	0.00211	0.01138
5	2683	7.3962	9.2452	6.1412	2.0492	8.1904
6	3050	7.4283	9.2850	3.7046	1.9582	5.6628
7	3049	5.6136	7.0176	1.7065	0.63027	2.33677
8	3048	5.7954	7.2441	0.9389	0.0891	1.028
9	2655	6.1104	7.6381	0.001	0.00001	0.00101
10	4323	1.3915	1.7397	0.001	0.00010	0.0011
11	4322	1.5732	1.9665	0.001	0.00001	0.00101
12	4321	1.8109	2.2637	0.001	0.00001	0.00101
13	4080	2.7881	3.4852	0.001	0.00003	0.00103
14	4063	3.3701	4.2127	0.000	0.000	0
15	3051	3.9057	4.8823	0.000	0.000	0

Table 8.2 Cumulative Fatigue Usage for n = 10^6& n = 10^4 cycles

ISSN No: 2348-4845
International Journal & Magazine of Engineering, Technology, Management and Research
A Peer Reviewed Open Access International Journal

From the table 8.2, it was determined that sever fatigue damage occurs at root TE edge of the turbine blade. At these node sections the cumulative fatigue usage gradually decreases as 8.1904, 5.6628, 2.3367 etc.,

Number of cycles used

Cumulative fatigue usage (CFU) = $n_1/N_1 + n_2/N_2$

Event 1, n = 10^7 cycles and Event 2, n = 10^4 cycles:

SL.NO	NODE	ALTERNATIVE STRESS (MPa)		CYCLES USED/ALLOWED		CFU
		EVENT 1	EVENT 2	n_1/N_1	n_2/N_2	
1	2653	2.5193	3.1492	2.0268	0.351	0.8231
2	4504	4.6125	5.7657	1.7505	0.3943	0.56935
3	4503	3.1617	3.1617	0.0100	0.002	0.003
4	4502	3.7396	4.6746	0.0926	0.0211	0.03037
5	2683	7.3962	9.2453	16.1412	20.492	26.6332
6	3050	7.4280	9.2859	12.7046	19.582	23.2866
7	3049	5.6136	7.0172	9.7065	6.3027	8.0092
8	3048	5.7951	7.2444	6.9389	0.891	1.8299
9	2655	6.1104	7.6381	0.0100	0.0001	0.0011
10	4323	1.3912	1.7397	0.0100	0.0001	0.0011
11	4322	1.5732	1.9665	0.0100	0.0001	0.0011
12	4321	1.8109	2.2637	0.0100	0.0001	0.0011
13	4080	2.7881	3.4852	0.0100	0.0003	0.0013
14	4063	3.3701	4.2127	0.0000	0	0
15	3051	3.9057	4.8882	0.0000	0	0

Table 8.3 Cumulative Fatigue Usage for n = 10^7& n = 10^4 cycles

From the table 8.3, it was determined that sever fatigue damage occurs at root TE edge of the turbine blade. Due to this High cyclic fatigue failure also starts near the blade's root LE. Where cumulative fatigue usage is 26.6332, 23.2866, 8.0092...etc.

Number of cycles used

Cumulative fatigue usage (CFU) = $n_1/N_1 + n_2/N_2$

Event 1, n = 10^8 cycles and Event 2, n = 10^4 cycles:

SL.NO	NODE	ALTERNATIVE STRESS (MPa)		CYCLES USED/ALLOWED		CFU
		EVENT 1	EVENT 2	n_1/N_1	n_2/N_2	
1	2653	2.5193	3.1492	2.0268	3.51	3.9821
2	4504	4.6125	5.7657	1.7505	3.943	4.11805
3	4503	3.1617	3.1617	0.0100	0.02	0.021
4	4502	3.7396	4.6746	0.0926	0.211	0.22027
5	2683	7.3962	9.2453	16.1412	204.92	211.0612
6	3050	7.4280	9.2859	12.7046	195.82	199.5246
7	3049	5.6136	7.0172	9.7065	63.027	64.7335
8	3048	5.7951	7.2444	6.9389	8.91	9.8489
9	2655	6.1104	7.6381	0.0100	0.001	0.002
10	4323	1.3912	1.7397	0.0100	0.001	0.002
11	4322	1.5732	1.9665	0.0100	0.001	0.002
12	4321	1.8109	2.2637	0.0100	0.001	0.002
13	4080	2.7881	3.4852	0.0100	0.003	0.004
14	4063	3.3701	4.2127	0.0000	0	0
15	3051	3.9057	4.8882	0.0000	0	0

Table 8.4 Cumulative Fatigue Usage for n = 10^8& n = 10^4 cycles

From the table 8.4, it was determined that sever fatigue damage occurs at root TE edge of the turbine blade. Due to this High cyclic fatigue failure also starts near the blade's root LE. Where cumulative fatigue usage is 211.06, 199.52, 64.73, etc.

From the results, at node 2563 the mean stress effects on fatigue life of the blade is determined and various curves for the location proved at this conditions the blade has infinite life.

Alternative stress	σ_a	=	2.519 MPa
Mean stress	σ_m	=	875 MPa
Endurance limit	σ_e	=	522 MPa
Yielding stress	σ_y	=	880 MPa
Ultimate stress	σ_u	=	950 MPa

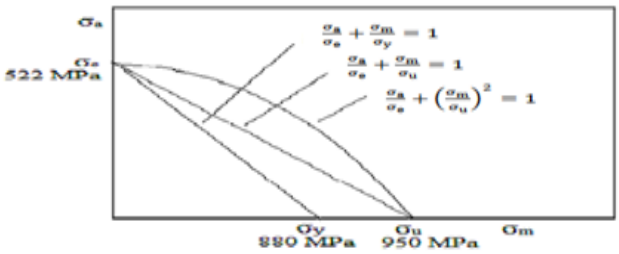

Figure 8.1 Soderberg, Goodman & Gerber curves for the model

CONCLUSION

The combination of event 1, load 1 and event 1, load 2 produces alternating stress intensity at various node point. In which the model was subjected to 10^6, 10^7,and 10^8cycles while from the S-N table, the maximum number of cycles allowed at various intensity shown in the Table 8.2 - 8.4.The combination of event 2, load 1 and event 2, load 2 produces alternating stress intensity at various node point. In which the model was subjected to 10^4 cycles while from the S-N table, the maximum number of cycles allowed at various intensity shown in the Table 8.2 - 8.4.The cumulative fatigue usage of the various nodes also shown in the table. Since the cumulative fatigue damage was calculated by the ratio of cycles used/cycles allowed.

From Miner Rule,The failure occurs when the cumulative fatigue usage value exceeds 1.From the

ISSN No: 2348-4845
International Journal & Magazine of Engineering, Technology, Management and Research
A Peer Reviewed Open Access International Journal

results, it was found that the failure occurs at the leading and trailing edge of the turbine blade root, which is shown in table.

REFERENCES

[1]. R. O. Ritchie,S. Suresh,J. W. Hutchinson,W. W. Milligan'High-Cycle Fatigue and Time-Dependent Failure in Metallic Alloys for Propulsion SystemsAfosr F49620-96-1-0478'

[2]. JianfuHou , Bryon J. Wicks and Ross A. Antoniou (2000),'An investigation of fatigue failures of turbine blades in a gasturbine engine by mechanical analysis', Elsevier Science Ltd

[3]. Kyo-Soo Song, Seon-Gab Kim, Daehan Jung and Young-Ha Hwang(2006)'Analysis of the fracture of a turbine blade on a turbojet engine' Engineering Failure Analysis 14 ,877–883

[4]. J.O. Peters, R.O. Ritchie (2001) 'Foreign-object damage and high-cycle fatigue of Ti–6Al–4V' Materials Science and Engineering A319–321 (2001) 597–601.

[5]. R.K. Nallaa, J.P. Campbell b, R.O. Ritchie(2001)'Mixed-mode, high-cycle fatigue-crack growth thresholds in Ti–6Al–4V: Role of small cracks' International Journal of Fatigue 24 (2002) 1047–1062.